

## Thyroid hormone stimulates hepatic lipid catabolism via activation of autophagy

Rohit Anthony Sinha, ... , Mitchell A. Lazar, Paul M. Yen

*J Clin Invest.* 2012;122(7):2428-2438. <https://doi.org/10.1172/JCI60580>.

Research Article

Metabolism

For more than a century, thyroid hormones (THs) have been known to exert powerful catabolic effects, leading to weight loss. Although much has been learned about the molecular mechanisms used by TH receptors (TRs) to regulate gene expression, little is known about the mechanisms by which THs increase oxidative metabolism. Here, we report that TH stimulation of fatty acid  $\beta$ -oxidation is coupled with induction of hepatic autophagy to deliver fatty acids to mitochondria in cell culture and in vivo. Furthermore, blockade of autophagy by autophagy-related 5 (ATG5) siRNA markedly decreased TH-mediated fatty acid  $\beta$ -oxidation in cell culture and in vivo. Consistent with this model, autophagy was altered in livers of mice expressing a mutant TR that causes resistance to the actions of TH as well as in mice with mutant nuclear receptor corepressor (NCoR). These results demonstrate that THs can regulate lipid homeostasis via autophagy and help to explain how THs increase oxidative metabolism.

Find the latest version:

<https://jci.me/60580/pdf>





# Thyroid hormone stimulates hepatic lipid catabolism via activation of autophagy

Rohit Anthony Sinha,<sup>1</sup> Seo-Hee You,<sup>2</sup> Jin Zhou,<sup>1</sup> Mobin M. Siddique,<sup>1</sup> Boon-Huat Bay,<sup>3</sup> Xuguang Zhu,<sup>4</sup> Martin L. Privalsky,<sup>5</sup> Sheue-Yann Cheng,<sup>4</sup> Robert D. Stevens,<sup>6</sup> Scott A. Summers,<sup>1,6</sup> Christopher B. Newgard,<sup>6</sup> Mitchell A. Lazar,<sup>2</sup> and Paul M. Yen<sup>1,6</sup>

<sup>1</sup>Cardiovascular and Metabolic Disorders Program, Duke-NUS Graduate Medical School, Singapore. <sup>2</sup>Division of Endocrinology, Diabetes, and Metabolism, Department of Medicine, The Institute for Diabetes, Obesity, and Metabolism, Perelman School of Medicine at the University of Pennsylvania School of Medicine, Philadelphia, Pennsylvania, USA. <sup>3</sup>Department of Anatomy, Yong Loo Lin School of Medicine, Department of Anatomy, National University of Singapore, Singapore. <sup>4</sup>Laboratory of Molecular Biology, Center for Cancer Research, National Cancer Institute, Bethesda, Maryland, USA. <sup>5</sup>Department of Microbiology, UCD, Davis, California, USA. <sup>6</sup>Sarah W. Stedman Nutrition and Metabolism Center, Departments of Medicine and Pharmacology and Cancer Biology, Duke University Medical Center, Durham, North Carolina, USA.

**For more than a century, thyroid hormones (THs) have been known to exert powerful catabolic effects, leading to weight loss. Although much has been learned about the molecular mechanisms used by TH receptors (TRs) to regulate gene expression, little is known about the mechanisms by which THs increase oxidative metabolism. Here, we report that TH stimulation of fatty acid  $\beta$ -oxidation is coupled with induction of hepatic autophagy to deliver fatty acids to mitochondria in cell culture and in vivo. Furthermore, blockade of autophagy by autophagy-related 5 (ATG5) siRNA markedly decreased TH-mediated fatty acid  $\beta$ -oxidation in cell culture and in vivo. Consistent with this model, autophagy was altered in livers of mice expressing a mutant TR that causes resistance to the actions of TH as well as in mice with mutant nuclear receptor corepressor (NCoR). These results demonstrate that THs can regulate lipid homeostasis via autophagy and help to explain how THs increase oxidative metabolism.**

## Introduction

Thyroid hormones (THs) have been known to stimulate basal metabolic rate for over a century (1, 2). Subsequent studies showed that THs induced energy expenditure in response to increased caloric intake (3). Later, several intracellular processes were shown to be involved in the calorogenic effects of THs. These included increased ATP expenditure due to increased Na<sup>+</sup>/K<sup>+</sup>-ATPase activity to maintain ion gradients in various tissues (4, 5) as well as reduced efficiency of ATP synthesis, particularly through the induction of uncoupling proteins (UCPs), which cause proton leakage in the electron transport chain of the mitochondria of target tissues (6, 7). However, despite these advances in our understanding of THs on cellular metabolism, none of these proposed mechanisms appears to be dominant. Currently, little is known about other mechanisms that might be utilized by THs to regulate energy consumption within the cell. This is particularly true for the events involved in the delivery of fatty acids to mitochondria, a necessary step in converting stored intracellular triglyceride fuel into ATP.

The active form of TH, 3,3',5-triiodo-L-thyronine (T<sub>3</sub>), is a critical regulator of cellular and tissue metabolism throughout the body. It controls gene expression in target tissues by binding to its cognate nuclear receptors (TR $\alpha$  and TR $\beta$ ), which are ligand-inducible transcription factors. In the presence of T<sub>3</sub>, TH receptors (TRs) bind to TH response elements in the promoters of target genes and form coactivator complexes containing histone acetyltransferase activity to activate transcription (8). In the absence of T<sub>3</sub>, TRs recruit corepressors such as NCoR and silencing mediator of retinoid and thyroid receptors (SMRT), which together with transducin  $\beta$ -like protein 1 (TBL1) and histone deacetylase 3 (HDAC3)

form a complex with histone deacetylase activity on the promoters of target genes that repress basal transcription (9). At the metabolic level, T<sub>3</sub> exerts strong effects on hepatic carbohydrate and lipid metabolism during both anabolic and catabolic states. Lipid synthesis and storage are regulated by T<sub>3</sub> via increased expression of lipogenic genes such as fatty acid synthase (*FAS*), *Thrsp* (Spot 14), and acetyl-CoA-carboxylase (*ACCI*) (10, 11). In addition, prolonged T<sub>3</sub> treatment promotes the catabolism of fatty acids by increasing the expression and activity of *Cpt1 $\alpha$* , a rate-limiting enzyme for transport and  $\beta$ -oxidation of fatty acids in the mitochondria (12). Thus, catabolism of fatty acids is a cardinal metabolic feature of prolonged hyperthyroidism (13).

T<sub>3</sub> stimulates the shuttling of free fatty acids for delivery into the mitochondria (14). While this process is well described, the T<sub>3</sub>-regulated cellular pathways that lead to the generation of free fatty acids from stored lipid droplets in liver are not very well understood. Recently, autophagy of lipid droplets, termed "lipophagy," has been shown to be a major pathway of lipid mobilization in hepatocytes (15–17), and its inhibition has been linked to development of fatty liver and insulin resistance (18–20).

Here, we show that T<sub>3</sub> induces lipophagy in cultured liver cell lines. TH also induces hepatic autophagy in vivo coupled with ketogenesis and a lipolytic metabolomic profile. Moreover, TH stimulation of autophagy and lipid metabolism is TR dependent and modulated by NCoR corepressor activity. Our findings suggest that T<sub>3</sub> plays an important role in the regulation of hepatic autophagy, which is a critical step for the physiological mobilization and metabolism of fatty acids.

## Results

*TH (T<sub>3</sub>) induces autophagy in TR-expressing HepG2 cells.* To address the role of TH in hepatic autophagy in human liver, we studied the well-characterized HepG2 cell line, which retains many liver-spe-

**Authorship note:** Rohit Anthony Sinha and Seo-Hee You are co-first authors.

**Conflict of interest:** The authors have declared that no conflict of interest exists.

**Citation for this article:** *J Clin Invest.* 2012;122(7):2428–2438. doi:10.1172/JCI60580.

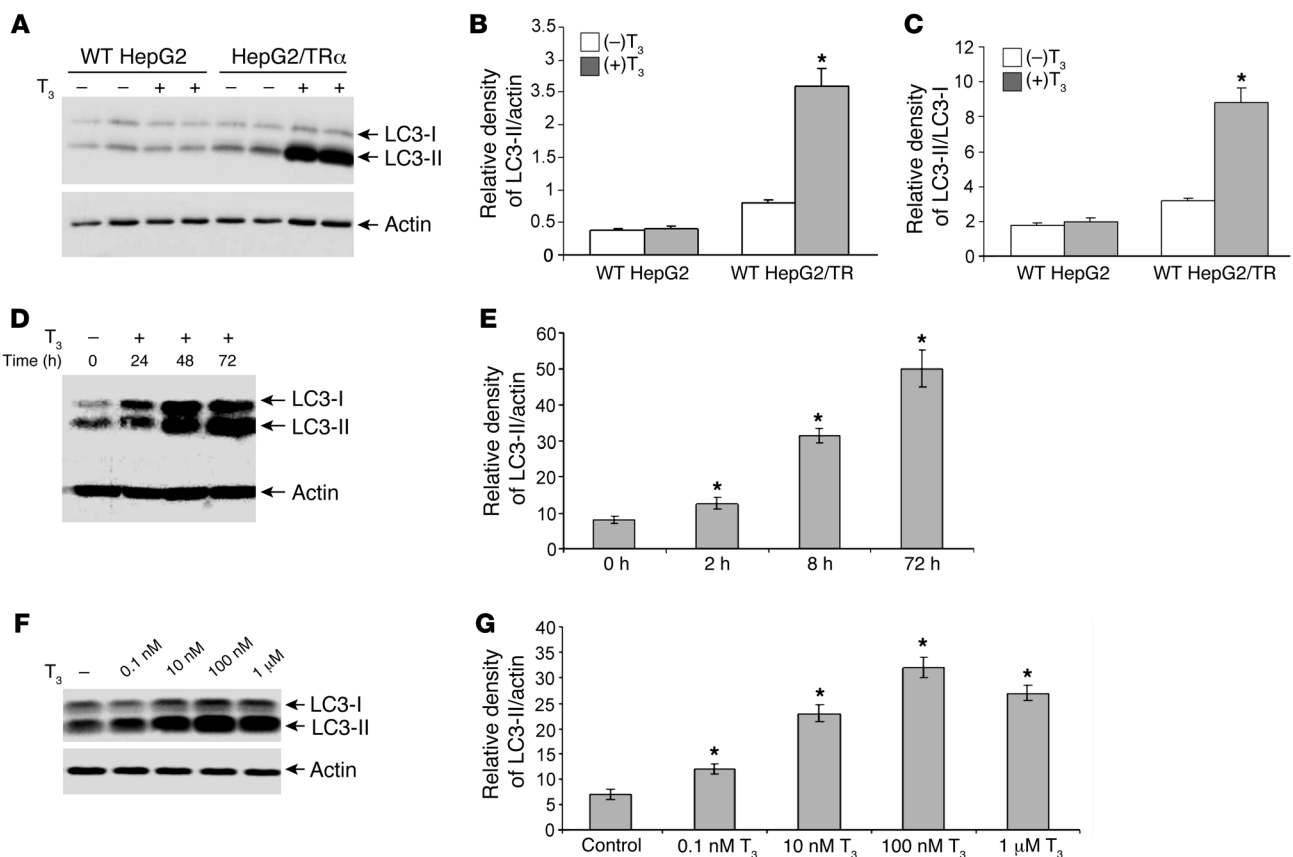


**Figure 1**

T<sub>3</sub> induces autophagy in hepatic cells expressing TRα. (A–C) Immunoblot and densitometric analysis of LC3-II levels in T<sub>3</sub>-treated HepG2 cells expressing TRα1 (HepG2/TRα) (n = 4; \*P < 0.05). (D and E) Time course of LC3-II accumulation in HepG2/TRα cells treated with 1 μM T<sub>3</sub> (n = 3; \*P < 0.05). (F and G) Dose response of LC3-II accumulation in HepG2/TRα cells treated with indicated concentrations of T<sub>3</sub> for 72 hours (n = 3; \*P < 0.05). Results are expressed as mean ± SEM.

cific metabolic functions (21). Since HepG2 cells have very low levels of TR proteins (22, 23), we also studied HepG2 cells expressing hTRα1 or hTRβ1 (HepG2/TRα, HepG2/TRβ). These cells previously were shown to be transcriptionally responsive to T<sub>3</sub> in transfection and microarray studies (24).

The phosphatidylethanolamine-conjugated form of LC3, LC3-II, is present in autophagosomes and thus is a commonly used marker of autophagy activation. We found that T<sub>3</sub> significantly increased LC3-II levels in HepG2/TRα cells (Figure 1, A and B). However, T<sub>3</sub> did not induce autophagy in WT HepG2 cells, suggesting that detectable TR expression was necessary for this effect to occur (Figure 1, A–C).

T<sub>3</sub> induction of autophagy was rapid, as it occurred as early as 24 hours (Figure 1, D and E) and was observed at T<sub>3</sub> concentrations as low as 0.1 nM (Figure 1, F and G), with an ED<sub>50</sub> in the nanomolar range consistent with the known binding affinity of TR (25).

Since it is possible that either induction of autophagy or inhibition of autophagosome clearance could account for the increase in LC3-II levels (26), we measured autophagic flux by comparing the generation of LC3-II by T<sub>3</sub> alone or in combination with chloroquine (CQ). CQ inhibits the acidification within lysosomes and endosomes and thus blocks the turnover and degradation of autophagosomes that fuse with them. CQ and T<sub>3</sub>

treatment significantly increased LC3-II levels compared with T<sub>3</sub> alone in cells (Figure 2, A–C). This accumulation of undegraded LC3-II after CQ treatment suggested that T<sub>3</sub> induction of LC3-II was due to increased autophagic flux. We also confirmed the increase in autophagic flux using tandem red fluorescent protein–GFP-tagged (RFP–GFP-tagged) LC3 plasmid (27), which showed an increase in the number of both autophagosomes (yellow dots) and autolysosomes (red dots) following T<sub>3</sub> treatment (Supplemental Figure 1, A and B; supplemental material available online with this article; doi:10.1172/JCI60580DS1). The presence of the red dots indicates that LC3 is present within lysosomes, since autophagosomes are able to fuse with lysosomes due to autophagic flux. We also tested the ability of T<sub>3</sub> to promote autophagy in several other hepatic cell lines, AML-12, Hep3B, and Huh7, that contain endogenous TRs at detectable protein levels (23, 28, 29). We observed that T<sub>3</sub> significantly increased LC3-II levels in these cells, further confirming that T<sub>3</sub> is proautophagic in hepatic cells (Figure 2, D and E).

T<sub>3</sub> induction of autophagy was also detected by the increased staining of LC3-II as punctate dots that are characteristic of autophagosomal membranes in the cytoplasm (Figure 3A). T<sub>3</sub> also increased cytoplasmic acridine orange (AO) staining, indicative of acidic vesicular organelle formation that is characteristic of

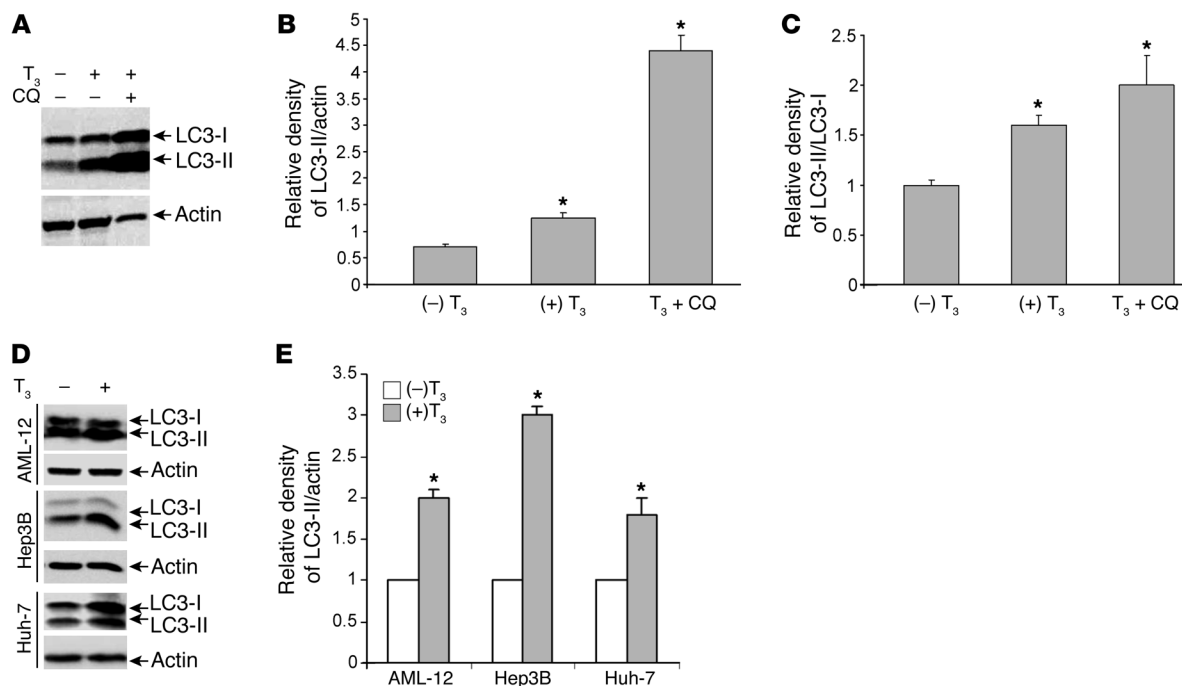


**Figure 2** T<sub>3</sub> stimulates autophagic flux and also induces autophagy in multiple hepatic cell lines. (A–C) Immunoblot and densitometric for LC3-II showing autophagic flux using HepG2/TRα cells treated with 1 μM T<sub>3</sub> and 50 μM CQ for 72 hours (n = 4; \*P < 0.05). (D and E) Immunoblot analysis of LC3-II levels in AML-12, Hep3B, and Huh7 cells upon 1 μM T<sub>3</sub> treatment for 72 hours showing increased autophagy (n = 3; \*P < 0.05). Results are expressed as mean ± SEM.

autophagy and autolysosomal activity (Figure 3B and ref. 30). Additionally, T<sub>3</sub> stimulated cytoplasmic accumulation of monodansylcadaverine (MDC), which marks autolysosomes and lysosomes (ref. 31 and Figure 3B). These results demonstrating increased lysosomal acidification by T<sub>3</sub> are consistent with earlier findings that showed that T<sub>3</sub> induced lysosomal activity in mice (32).

*T<sub>3</sub> promotes lipophagy in hepatic cells.* To further characterize the autophagy induced by T<sub>3</sub>, we performed transmission EM of HepG2/TRα cells. This revealed an increased number of autophagosomes and lysosomes as well as increased formation of large lipid droplets in T<sub>3</sub>-treated cells (Figure 4, B–F). The latter likely are due to the rapid induction of fatty acid synthesis by T<sub>3</sub> (Supplemental Figure 2) that occurs before the switch to fatty acid oxidation seen after chronic T<sub>3</sub> treatment (13). Higher magnification images revealed sequestration of lipid within double membranous autophagosomes and autolysosomes that are characteristic of lipophagy (Figure 4, D–F). Moreover, increased staining of lipophilic BODIPY dye was observed after T<sub>3</sub> treatment, and its overlap with LC3 confirms induction of lipophagy by T<sub>3</sub> (Figure 4G). We also observed that T<sub>3</sub> increased LC3 mRNA (2.1-fold) as well as *Cpt1α* mRNA (2.85-fold) in cells. Similar to the increased autophagy observed in HepG2/TRα cells, HepG2/TRβ cells also showed increased autophagosome formation and lipophagy by EM (Supplemental Figure 3, A and B). These results demonstrate that T<sub>3</sub>-mediated induction of hepatic lipophagy is not dependent upon the TR isoform being expressed in hepatic cells.

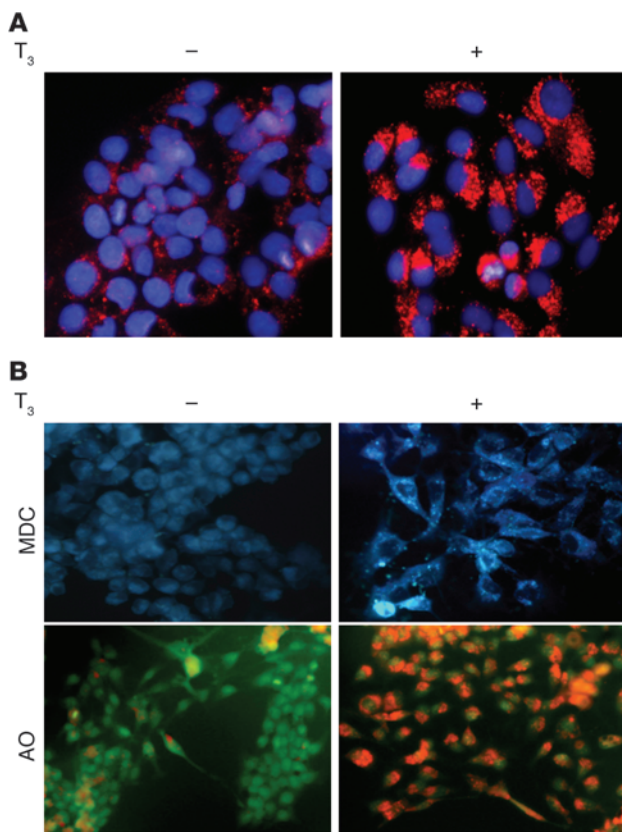
*T<sub>3</sub> promotes hepatic autophagy in vivo.* In order to assess the role of T<sub>3</sub> in the regulation of autophagy in vivo, we injected C57BL/6 mice with T<sub>3</sub> (10 μg/100 g BW) daily for 3 days. In these hyper-

thyroid mice, T<sub>3</sub> increased hepatic LC3-II and decreased p62 protein levels in mouse livers, indicative of autophagy (Figure 5, A–D). The downregulation of p62 protein was likely secondary to increased autophagic flux, as *p62* gene expression was unchanged (data not shown).

EM images showed increased hepatic lipid-containing autophagosomes and lysosomes, with a concomitant increase in the number of hepatic mitochondria in T<sub>3</sub>-treated mice, suggesting mitochondrial biogenesis and an increase in oxidative phosphorylation (Figure 5, E–I, and ref. 33). We also found a significant increase in the expression of *PGC1α* mRNA (2.87 ± 0.2-fold), which is consistent with the increase in mitochondrial number (data not shown).

*T<sub>3</sub>-regulated autophagy is TR dependent.* To further study the role of TR in T<sub>3</sub>-mediated autophagy, we used a well-characterized mouse model (34) in which the normal TRβ allele is replaced by the TRβPV mutant allele originally identified in a patient with resistance to TH (RTH) (35). The encoded mutant receptor has markedly decreased T<sub>3</sub> binding and transcriptional activity while maintaining its ability to bind to the thyroid hormone response elements (TRE) and thus functions as a dominant negative on WT TR (34). These TRβPV mice have defective β-oxidation of lipids and develop fatty livers (36). Remarkably, TRβPV mice had reduced LC3-II levels compared with WT euthyroid littermate controls despite having elevated circulating serum T<sub>3</sub> levels (ref. 34 and Figure 6A). The TRβPV mice also had increased hepatic p62 accumulation, similar to the levels observed in hypothyroid WT mice (Figure 6B). These data strongly suggest that the induction of liver autophagy by T<sub>3</sub> is mediated by TR and not via pathways involving other cellular proteins (37).



**Figure 3**

$T_3$  stimulates autophagosomal and lysosomal activity in hepatic cells. (A) LC3 immunostaining. Punctate staining shows autophagosome formation in cells treated with 1  $\mu\text{M}$   $T_3$  for 72 hours. (B) Lysosomal acidification visualized using MDC and AO in HepG2/TR $\alpha$  cells treated with 1  $\mu\text{M}$   $T_3$  for 72 hours.

*T<sub>3</sub>-induced lipophagy regulates  $\beta$ -oxidation of fatty acids in hepatic cells.* Singh et al. previously showed that lipophagy was causally linked to  $\beta$ -oxidation of fatty acids in hepatocytes (15). To determine whether lipophagy stimulated by  $T_3$  also induced fatty acid oxidation, we used autophagy-related 5 (ATG5) siRNA to inhibit autophagy in HepG2/TR $\alpha$  cells treated with oleic acid to maximize  $\beta$ -oxidative flux. We then measured the levels of the end product of fatty acid  $\beta$ -oxidation,  $\beta$ -hydroxybutyrate, in the medium. These cells showed a significant increase in  $\beta$ -hydroxybutyrate release following  $T_3$  stimulation when transfected with a control siRNA; however, this increase was completely abolished in the presence of ATG5 siRNA (Figure 7). The effect of ATG5 knockdown on autophagy also was confirmed by the expected changes in LC3-II levels (Figure 7), indicating that autophagy plays a major role in  $T_3$ -induced  $\beta$ -oxidation of fatty acids in hepatic cells.

*T<sub>3</sub>-mediated autophagy is tightly coupled with  $\beta$ -oxidation of fatty acids in vivo.* We next investigated the contribution of autophagy in  $T_3$ -mediated fatty acid  $\beta$ -oxidation in the livers of living mice. Mice were subjected to tail-vein injection of ATG5 siRNA, which led to a marked reduction in hepatic ATG5 protein (Figure 8A) and mRNA (data not shown) relative to mice injected with control siRNA after 72 hours.  $T_3$  treatment caused increased LC3-II levels in livers of mice injected with control siRNA and increased serum

hydroxybutyrate levels (Figure 8, A–C). In contrast, livers of  $T_3$ -treated mice injected with ATG5 siRNA did not exhibit increased autophagy or increased circulating levels of  $\beta$ -hydroxybutyrate (Figure 8, A–C). Taken together with our previous findings in hepatic cells, these results show that  $T_3$ -mediated  $\beta$ -oxidation of fatty acids is tightly coupled with the effect of the hormone in inducing autophagy in liver. These findings also suggest that autophagy is an important physiological mechanism for  $T_3$  stimulation of  $\beta$ -oxidation of fatty acids.

*NCoR modulates  $T_3$ -mediated autophagy and lipid catabolism in liver.* TH action involves TR interaction with nuclear receptor corepressor (NCoR) (38–40). We examined the role of NCoR in  $T_3$ -mediated autophagy in vivo by studying mice (NCoR DADm mice) expressing a mutant NCoR that is expressed at normal levels but does not bind to HDAC3, a critical component of the corepressor complex (40). In both the WT and NCoR DADm mice, a progressive increase was observed in LC3-II levels in the hypothyroid, euthyroid, and hyperthyroid mice. However, LC3-II levels were higher in the hypothyroid NCoR DADm mice than in the WT littermates (Figure 9, A and B). In addition, although  $T_3$  stimulated LC3-II levels in both NCoR DADm and WT mice, the LC3-II levels were attenuated in the NCoR DADm mice compared with WT mice (Figure 9, A and B). These findings suggest a role for NCoR in the induction of autophagy by  $T_3$ .

*Both  $T_3$  and NCoR modulate the hepatic acylcarnitine profiles.* In order to better understand how  $T_3$  effects on autophagy have an impact upon  $\beta$ -oxidation of fatty acids in the liver, we analyzed the levels of a broad array of acylcarnitines in livers of WT and NCoR DADm mice under hypothyroid, euthyroid, and hyperthyroid conditions by tandem mass spectrometry. The levels of various acylcarnitines reflected the levels of cognate acyl-CoAs generated by oxidation of fatty acids and other fuels within the mitochondria. Our studies showed that medium-chain acylcarnitines (C8, C10) increased by similar amounts in both euthyroid and hyperthyroid mice compared with hypothyroid mice (control and TH vs. Per/MMI) (Figure 9C). Additionally, NCoR DADm mice had concentrations of medium-chain acylcarnitines similar to those of WT mice under all 3 conditions (Figure 9C). On the other hand, long-chain acylcarnitines (C16, C18) increased in hyperthyroid mice compared with euthyroid and hypothyroid mice, and the increase in long-chain acylcarnitines was sharply attenuated in hyperthyroid NCoR DADm mice (Figure 9D). Finally, short-chain acylcarnitines such as acetyl (C2) and propionyl (C3) were largely unaffected by thyroid status, but were sharply reduced in NCoR DADm mice only under hyperthyroid conditions (Supplemental Figure 4A). The overall picture that emerges is one of TH-induced activation of autophagy/lipophagy, increased delivery of long-chain fatty acyl CoAs/acylcarnitines to the mitochondria, and increased rates of fatty acid oxidation. The graded increase in medium-chain acylcarnitines under hypothyroid, euthyroid, and hyperthyroid conditions may indicate increased substrate entry into the  $\beta$ -oxidative pathway. In hyperthyroid mice, the rate of delivery of acylcarnitines may saturate the  $\beta$ -oxidative system, contributing to the accumulation of long-chain acylcarnitines under these conditions. These effects were attenuated in hyperthyroid NCoR DADm mice, perhaps due to a decrease in autophagy-mediated lipolysis in these animals.

The expression of hepatic lipase (*LIPC*) was significantly downregulated in hypothyroid WT and NCoR DADm mice, whereas it did not significantly change in hyperthyroid mice (Supplemental Figure 4, B and C). *ATGL* levels were significantly downregulated

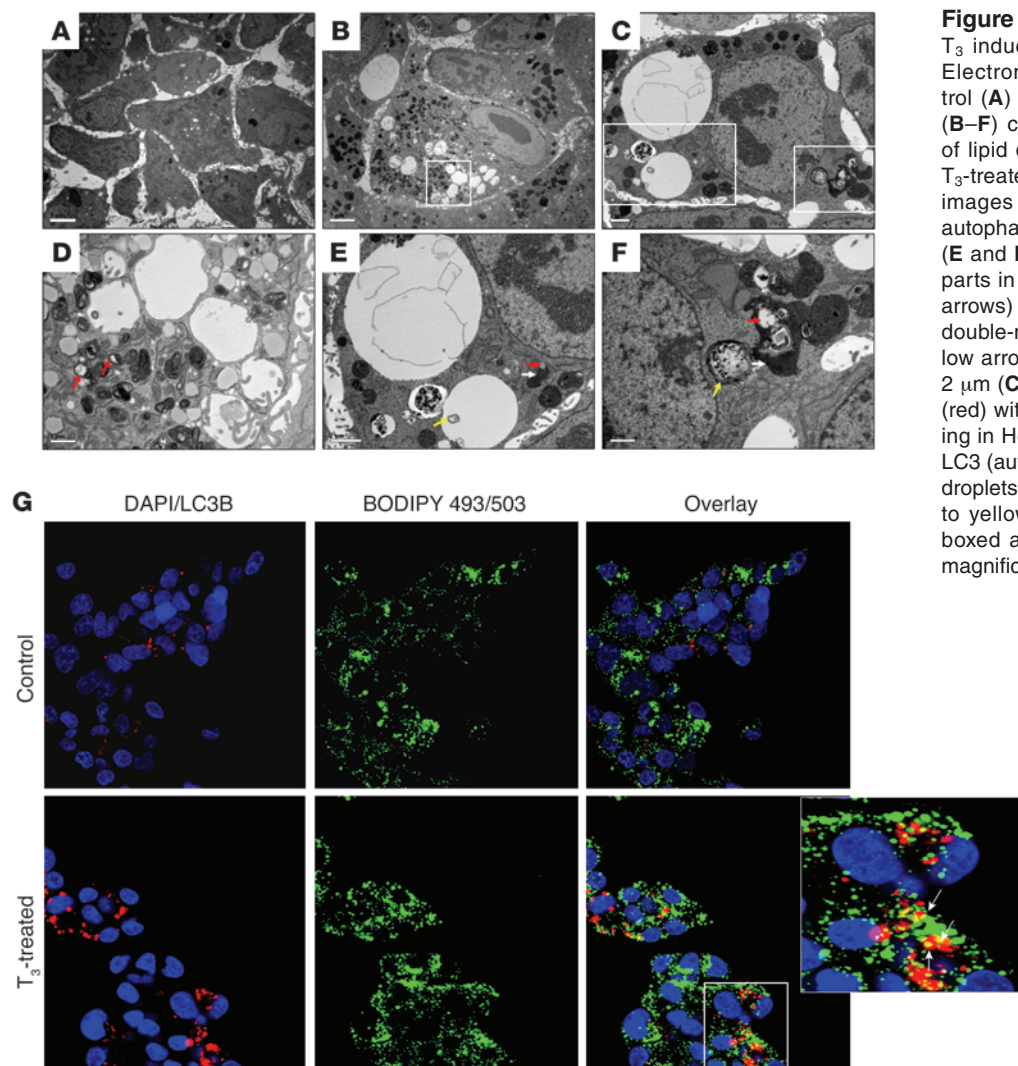


**Figure 4**  
 $T_3$  induces “lipophagy” in hepatic cells. Electron micrograph of untreated control (A) and  $T_3$ -treated HepG2/TR $\alpha$  cells (B–F) cells. Note the increased number of lipid droplets and autophagosomes in  $T_3$ -treated cells. (D) Higher magnification images of the boxed area in B showing autophagosomes with lipids (red arrows). (E and F) Magnified images of the boxed parts in C showing autolysosomes (white arrows) containing lipids (red arrows) and double-membrane autophagosomes (yellow arrows). Scale bars: 5  $\mu\text{m}$  (A and B), 2  $\mu\text{m}$  (C and E); 1  $\mu\text{m}$  (D and F). (G) LC3 (red) with BODIPY 493/503 (green) staining in HepG2/TR $\alpha$  cells. Colocalization of LC3 (autophagosomes) and BODIPY (lipid droplets) is shown by white arrow pointing to yellow spots in the digitally enlarged boxed area ( $\times 2.5$  digital zoom). Original magnification,  $\times 40$ .

only in hypothyroid NCoR DADm mice, whereas they remained unchanged in WT mice. *Cpt1a* mRNA levels remained largely unchanged, whereas *ACO* levels were decreased in hyperthyroid WT mice (Supplemental Figure 4, B and C).

*Microarray pathway analysis confirms that  $T_3$  stimulates lipid catabolism pathways in WT but not NCoR DADm mice.* We also performed microarray analyses of hepatic target genes induced by  $T_3$  in WT and NCoR DADm mice. Interestingly, pathway analysis of the differentially expressed genes showed that  $T_3$  induced pathways of lipid and amino acid catabolism pathways (Supplemental Figure 5, A and B). Moreover, these effects were dependent on NCoR-HDAC3 recruitment, as the effects of hyperthyroidism on the pathways regulating lipid and amino acid catabolism were not ranked in NCoR DADm mice (Supplemental Figure 5, A and B).

**Discussion**

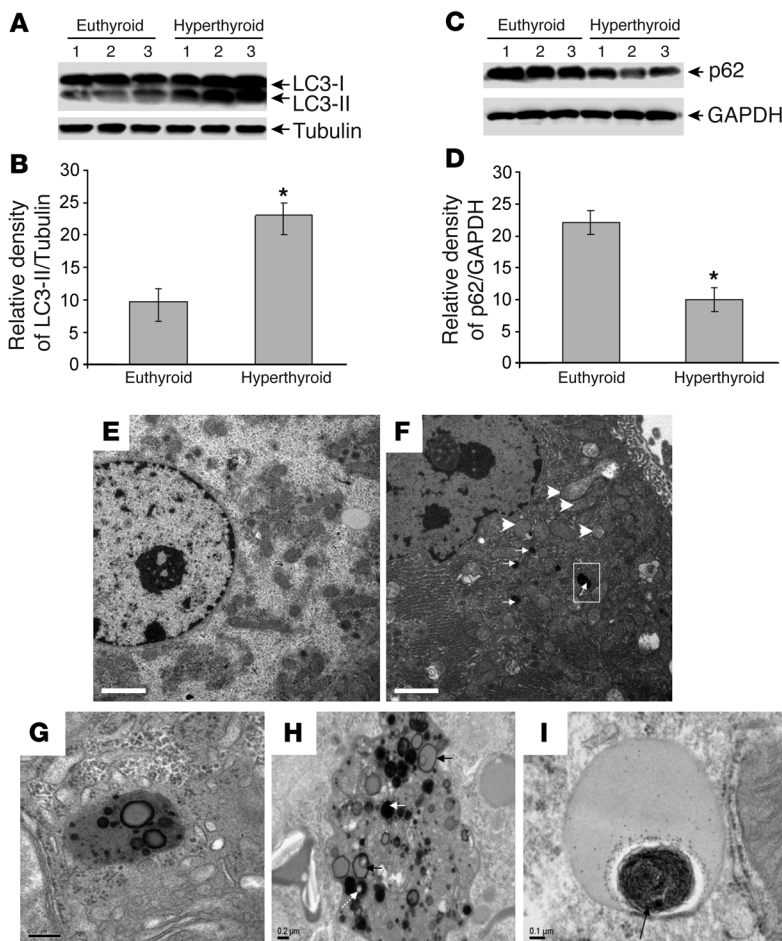
TH is well known as a metabolic regulator of energy expenditure through activation of  $\beta$ -oxidation of fatty acids in mammals (41). However, the precise mechanism of this effect has never been revealed. Here we have demonstrated an action of  $T_3$  in promoting lipophagy in both human hepatic cells in vitro and mouse liver in

vivo. This lipophagy was coupled with clear effects of  $T_3$  stimulation in altering the levels of a broad array of hepatic lipid-related metabolites, consistent with a key role of  $T_3$  as important regulator of the delivery of fatty acids to mitochondria and their metabolism.

Autophagy is a stress-induced catabolic process involving lysosome fusion that is conserved in all eukaryotes. During periods of starvation, autophagy degrades cytoplasmic materials to produce amino acids and fatty acids that can be used to synthesize new proteins or generate ATP for cell survival (42). Derangement of autophagic response has been implicated in several pathologic hepatic conditions, such as ischemia, reperfusion, viral infections, acute injury,  $\alpha 1$ -antitrypsin deficiency, hepatocellular carcinoma, alcoholic liver disease, and nonalcoholic fatty liver disease (NAFLD) (20, 43, 44). Hormonal regulation of hepatic autophagy by glucagon and insulin has been described previously (43). Recently, a previously unknown function for autophagy leading to the degradation of intracellular lipid droplets was described in hepatocytes and termed “lipophagy.” This process is now believed to provide substrate for  $\beta$ -oxidation of fatty acids (15).

*$T_3$  induces lipophagy in hepatocytes.* Several different lines of investigation presented here demonstrate  $T_3$ -mediated autophagy



**Figure 5**

$T_3$  induces hepatic autophagy *in vivo*. (A and B) Immunoblot and densitometric analysis of LC3-II levels in euthyroid and hyperthyroid mice injected with  $10 \mu\text{g } T_3/100 \text{ g BW}$  for 3 days ( $n = 3$ ;  $*P < 0.05$ ). (C and D) Immunoblot and densitometric analysis of p62 levels in euthyroid and hyperthyroid mice ( $n = 3$ ;  $*P < 0.05$ ). Results are expressed as mean  $\pm$  SEM. EM showing livers obtained from control (E) and hyperthyroid (F–I) mice injected with  $10 \mu\text{g } T_3/100 \text{ g BW}$  for 3 days. White arrowheads in F denote increased number of mitochondria in hyperthyroid mouse liver, and white arrows show autolysosomes. (G) Magnified image of the boxed area in F showing double-membrane lipid droplets inside autolysosomes. (H) Autophagic vesicle containing several lysosomes (white arrows) and lipid droplets (black arrow). (I) Autophagosome inside a large lipid droplet in hepatocyte from hyperthyroid mouse liver. Scale bars:  $2 \mu\text{m}$  (E and F);  $0.2 \mu\text{m}$  (G and H);  $0.1 \mu\text{m}$  (I).

agy, including immunodetection of LC3-II and p62, lysosomal staining showing increased acidification, tandem RFP-GFP-LC3 fluorescence, and EM evidence of lipophagy. Interestingly,  $T_3$ -treated cells exhibited an increased number of large lipid droplets in the cytosol compared with a few small lipid droplets in the untreated cells. It is likely that  $T_3$  initially increased accumulation of triglycerides due to its known early effect on lipogenesis (13). Indeed, we found the levels of key target lipogenic enzymes such as *FAS* and *ACC* were slightly increased by  $T_3$  at 24 hours after treatment (Supplemental Figure 2). Furthermore, LC3-II itself may be a critical regulator of lipid droplet formation in hepatocytes (45). The dual ability of  $T_3$  to form lipid droplets and lipid-containing autophagosomes could serve as a dynamic process for fuel delivery while concomitantly reducing the amount of toxic free fatty acids in the cells. This may be even more relevant at the physiological level, since fatty acids that are generated by  $T_3$ -stimulated lipolysis in adipose tissue must also be metabolized by the liver. Thus, the ability of  $T_3$  to regulate lipophagy provides new insight into the mechanism of hormonal regulation of energy metabolism, as it directly links autophagy with  $\beta$ -oxidation. The low levels of p62 after  $T_3$  treatment also indicate that proteins, along with lipids, are cargo components of autophagic degradation that potentially could be involved in quality control within the cell. Additional work will be needed to better understand the mechanism of  $T_3$ -induced autophagy, although our current data point to the regulation of Akt and AMPK signaling,

both of which play critical roles in autophagy (our unpublished observations and ref. 46).

*$T_3$ -mediated autophagy is tightly coupled with  $\beta$ -oxidation of fatty acids in hepatic cells and *in vivo*.* We observed that  $T_3$ -mediated increases in autophagy and  $\beta$ -oxidation were decreased when we knocked down ATG5 expression by siRNA in hepatic cells. Similarly, we observed that delivery of ATG5 siRNA into living mice suppressed expression of ATG5 and decreased  $T_3$ -mediated autophagy to control levels in the livers of living mice. ATG5 siRNA injection also decreased serum  $\beta$ -hydroxybutyrate levels to control levels. These hepatic cell and *in vivo* experiments demonstrate that autophagy is necessary for the  $T_3$ -mediated stimulation of fatty acid  $\beta$ -oxidation. Moreover, these 2 processes are tightly coupled. Our *in vivo* experiments also highlight the important role of autophagy in  $\beta$ -oxidation and ketone body production at the physiological level.

*TR is required for autophagy.* We found that TR is required for TH-induced autophagy in HepG2 cells, which was further borne out by reduced lipophagy in mice that are resistant to TH. This reduced autophagy occurs even in the face of markedly elevated circulating  $T_3$  concentrations in the TR $\beta$ PV mice. Indeed, our findings suggest that the lack of  $T_3$  binding and dominant negative activity of the TR $\beta$ PV mutation contribute to the loss of autophagy in the TR $\beta$ PV mouse livers and may partially explain their defective  $\beta$ -oxidation rates and fatty liver phenotype (36). While TR is necessary for  $T_3$ -mediated autophagy, it still is formally possible that the TR effects could be nongenomic, since sev-

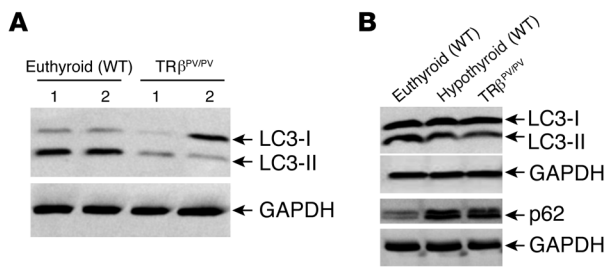


**Figure 6**  
 In vivo regulation of hepatic autophagy is TR dependent. (A) Immunoblot showing LC3-II levels in WT euthyroid and TRβPV/PV mice. (B) Immunoblot showing LC3-II and p62 levels in (2 to 3 months old) euthyroid mice, hypothyroid mice (fed with a low-iodine diet supplemented with 0.15% propylthiouracil [Harlan Teklad] for 35 days, and TRβPV/PV mice.

eral groups have reported cytosolic TR interaction with different protein kinases (37). However, our finding that the repression of autophagy observed in hypothyroidism did not occur in NCoR DADm mice argues for a nuclear effect of the TH via its TR.

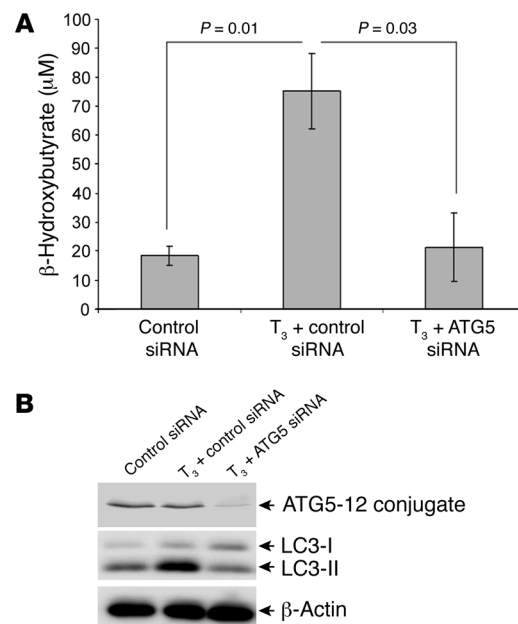
*NCoR-HDAC3 interaction regulates T<sub>3</sub>-mediated autophagy and lipid metabolism in vivo.* In the absence of TH, TR interacts with corepressors such as NCoR and SMRT that recruit HDACs to the promoters of target genes (8). NCoR is believed to preferentially control repression by unliganded TR in vivo. Consistent with this model, coexpression of dominant negative corepressors can interfere with the basal repression of target genes in mouse livers (38–40). Since transcriptional repression by unliganded TR-NCoR complex involves recruitment of HDAC3, several TH-responsive genes are modestly derepressed in the hypothyroid state in the livers of NCoR DADm mice, demonstrating an important role of the NCoR-HDAC3 interaction in basal repression (40). Similar findings have been reported in other dominant negative mutant NCoR mouse models (38, 39). Interestingly, we found that the repression of autophagy observed in hypothyroidism did not occur in NCoR DADm mice. Thus, it is possible that T<sub>3</sub>-regulated genes involved in autophagy that normally are repressed in hypothyroid WT mice may be derepressed in NCoR DADm mice. This is further supported by recent findings showing increased autophagy in hepatic cancer cells upon HDAC inhibition (47). In this connection, we also have observed that the HDAC inhibitor, trichostatin A, can induce autophagy in HepG2 cells (R.A. Sinha and P.M. Yen, unpublished observations).

Medium- and long-chain acylcarnitine levels in both groups of hyperthyroid mice correlated well with the LC3-II increase observed in the hyperthyroid mice, although the increase in long-chain acylcarnitines was sharply attenuated in the NCoR DADm mice. It is possible that the decreased autophagy and β-oxidation of fatty acids in the NCoR DADm mice may predispose them to develop hepatosteatosis. In this connection, a recent study showed that disruption of SMRT and nuclear receptor interaction led to insulin resistance and fatty liver (48). Similarly, the diabetes- and obesity-regulated gene (*DOR*), which is also a nuclear cofactor of TRs expressed abundantly in metabolically active tissues, has been shown to induce autophagy in drosophila and mammals (49). Thus, transcriptional cofactors, in addition to nuclear hormone receptors, may contribute to the development and phenotype of metabolic diseases and serve as potential therapeutic targets.

Although T<sub>3</sub> has been known to induce lipolysis, the mechanism by which it occurs is poorly understood. Our data suggest that T<sub>3</sub> increases the delivery of fatty acids to the mitochondria for β-oxidation via its induction of autophagy. Indeed, our cell culture and in vivo studies with ATG5 siRNA to knock down ATG5 expression and block autophagy showed that autophagy is critical for β-oxidation of fatty acids in the liver. These data and the observed increase in both long- and medium-chain acylcarnitines in our metabolomic studies suggest that lipophagy may be the key regulatory mechanism for increased β-oxidation of fatty acids early after T<sub>3</sub> treatment. In this connection, we did not observe any significant increase in the levels of hepatic lipases (*LIPC* and *ATGL*) or *Cpt1α* and *ACO* after acute T<sub>3</sub> treatment (14 hours), but it remains possible that additional mechanisms may contribute to the more prolonged effect of T<sub>3</sub>.

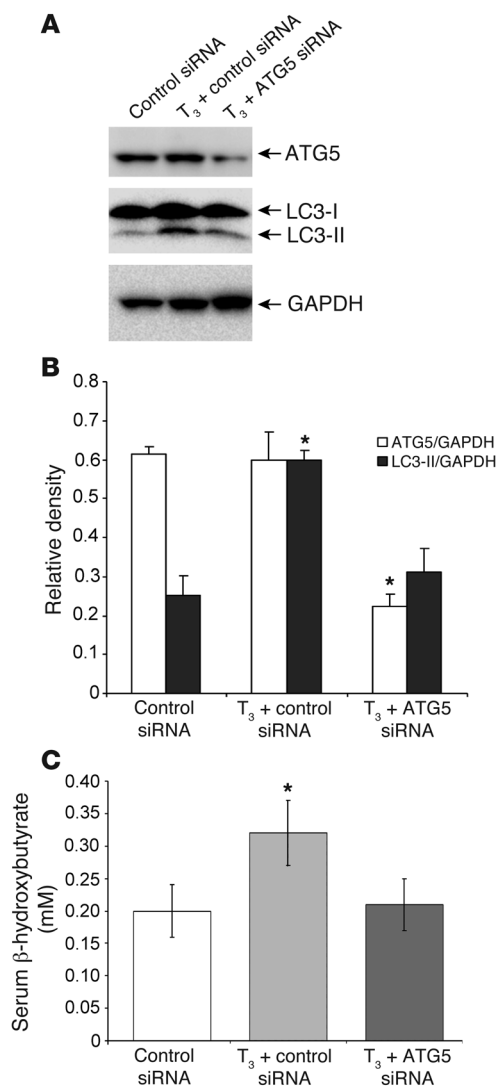
Our findings on T<sub>3</sub> regulation of lipophagy and β-oxidation of fatty acids may have relevance for patients with advanced stages of nonalcoholic steatohepatitis (NASH) in which activation of transcription by T<sub>3</sub> may be impaired in the liver (50). Indeed, it has been reported that TH deficiency is associated with increased incidence of NAFLD (51). However, it should be noted that many pathways in addition to autophagy contribute to hepatic lipid metabolism and the development of NAFLD (52).

Although our study has mostly focused on the protective aspects of T<sub>3</sub>-induced hepatic autophagy, prolonged autophagy can eventually lead to cell death (53). In particular, autophagic cell death may contribute to the hepatic damage and resultant liver failure sometimes observed during the rare clinical condition of extreme



**Figure 7**  
 Autophagy mediates fatty acid oxidation and ketosis by T<sub>3</sub> in hepatic cells. HepG2/TRα cells were transfected with either control siRNA or ATG5-specific siRNA. Cells then were cultured with oleic acid (0.5 mM) in the absence or presence of T<sub>3</sub> for the next 48 hours before harvesting. (A) β-Hydroxybutyrate concentrations in culture medium were measured along with (B) ATG5 and LC3-II protein levels, which were measured by Western blotting (n = 3/each group). Results are expressed as mean ± SEM.



**Figure 8**

T<sub>3</sub>-induced autophagy is tightly coupled with fatty acid  $\beta$ -oxidation in mouse liver in vivo. (A) Immunoblot of ATG5 and LC3-II from livers of representative mice treated with control siRNA or ATG5 siRNA in the absence or presence of T<sub>3</sub>. (B) Densitometric analyses of immunoblots of ATG5 and LC3-II in livers of mice treated with control siRNA or ATG5 siRNA in the absence or presence of T<sub>3</sub> ( $n = 4-5$ ; \* $P < 0.05$ ). Note that T<sub>3</sub> stimulation of LC3-II was blocked in the ATG5-knockdown mice. (C) Serum  $\beta$ -hydroxybutyrate levels from mice treated with control siRNA or ATG5 siRNA in the absence or presence of T<sub>3</sub> ( $n = 4-5$ ; \* $P < 0.05$ ). Note that  $\beta$ -hydroxybutyrate levels in ATG5-knockdown mice treated with T<sub>3</sub> returned to the same levels as those in mice treated with control siRNA alone. Results are expressed as mean  $\pm$  SEM.

dark cycle at 23°C with food and water available ad libitum. All cages contained shelters and nesting material. Hyperthyroidism and hypothyroidism were induced as indicated in the respective figures. Control mice were injected with PBS. The hypothyroid or hyperthyroid state of mice was confirmed by the determination of serum TH levels. Animals were sacrificed in CO<sub>2</sub> chambers, and blood was drawn by cardiac puncture. Livers were collected in liquid N<sub>2</sub> and subsequently used for protein and RNA isolation. During the course of the treatment, animals were monitored daily; general health and weight were examined and documented. TR $\beta$ PV and NCoR DADm mice have been described (34, 40).

**Cell culture.** HepG2, Hep3B, and Huh7 cells were maintained at 37°C in DMEM supplemented with 10% FBS using bicarbonate buffer and a 5% CO<sub>2</sub> atmosphere. HepG2 transformants expressing ectopic TR $\alpha$ 1, ectopic TR $\beta$ 1, or an empty plasmid control were generated as previously described using a G418 coselection methodology (24). AML-12 cells were grown at 37°C in DMEM/Ham's F-12 nutrient mixture with 10% FBS, 100 nM dexamethasone, and ITS (insulin, transferrin, and selenium [Invitrogen]). For all T<sub>3</sub> treatments, cells were grown for 3 days in DMEM containing 10% serum-stripped FBS before adding T<sub>3</sub> with or without other drugs at indicated concentrations and durations.

**RNA isolation and real-time PCR.** Total RNA was isolated using the Invitex Mini Kit (74106) (Invitex) or Trizol (Sigma-Aldrich). Total RNA (1  $\mu$ g) was reverse-transcribed by the iScript Select cDNA Synthesis Kit (170-8896) (Bio-Rad) in accordance with the manufacturer's instructions. Quantitative PCR (qPCR) was performed using the QuantiTect SYBR Green PCR Kit (QIAGEN) in accordance with the manufacturer's instructions. Actin levels were taken for normalization and fold change was calculated using 2<sup>- $\Delta\Delta$ C<sub>t</sub></sup>. Primer sequences are provided in Supplemental Table 1.

**MDC, AO, and BODIPY 493/503 staining.** Cells were grown on glass coverslips and treated with 1  $\mu$ M T<sub>3</sub> for 72 hours. Thereafter, the cells were incubated with 0.05 mM MDC or 1  $\mu$ g/ml AO (Sigma-Aldrich) for 15 minutes, fixed for 30 minutes at room temperature at 37°C, and immediately observed under fluorescence microscope. BODIPY 493/503 (Invitrogen) was dissolved in ethanol to give a stock of 1 mg/ml. Then 4% PFA-fixed cells were stained for 15 minutes at 1:1000 dilution, washed with PBS 3 times, and observed using an LSM710 Carl Zeiss confocal microscope.

**Western blotting.** Cells were lysed using mammalian lysis buffer (Sigma-Aldrich). An aliquot was removed, and protein concentrations were measured using the BCA Kit (Bio-Rad). Laemmli sample buffer was added to the remainder (composition: 250 mmol/l Tris, pH 7.4, 2% w/v sodium dodecyl sulfate, 25% v/v glycerol, 10% v/v 2-mercaptoethanol, and 0.01% w/v bromophenol blue), and samples were heated to 100°C for 5 minutes and stored at -80°C until analysis. Equal amounts of protein were separated by sodium dodecyl sulfate-polyacrylamide gel electrophoresis and transferred immediately onto polyvinylidene difluoride membranes (Bio-Rad) using 1 $\times$  Towbin buffer (25 mmol/l Tris, pH 8.8, 192 mmol/l glycine,

hyperthyroidism or "thyroid storm" (54). Therefore, it is likely that there is an optimal intrahepatic TH concentration that mediates autophagy to enable the liver to clear and metabolize cellular fuel stores in an efficient manner.

In conclusion, we have described a cellular action of TH to induce autophagy in mammalian hepatic cells both in vitro and in vivo. Our results underscore the importance of T<sub>3</sub> in not only regulating eumetabolic status, but also mobilizing and metabolizing stored lipids in the liver to provide the necessary fuel to maintain that state. These findings raise the possibility that T<sub>3</sub> or its analogs, through their proautophagic action, may be useful in the treatment or prevention of NAFLD and its associated complications.

## Methods

**Reagents.** T<sub>3</sub>, monodansylcadaverine (MDC), AO, oleic acid, anti-p62 antisera, and DAPI were from Sigma-Aldrich. Antibodies recognizing human LC3, actin, cleaved caspase-3, and GAPDH were from Cell Signaling Technology. Culture medium and serum were from Invitrogen. GFP-RFP-LC3 was a gift provided by T. Yoshimori (Osaka University, Osaka, Japan) (55).

**Animals.** Male C57BL/6 mice (2 to 3 months old) were purchased and housed in hanging polycarbonate cages under a 12-hour light/12-hour

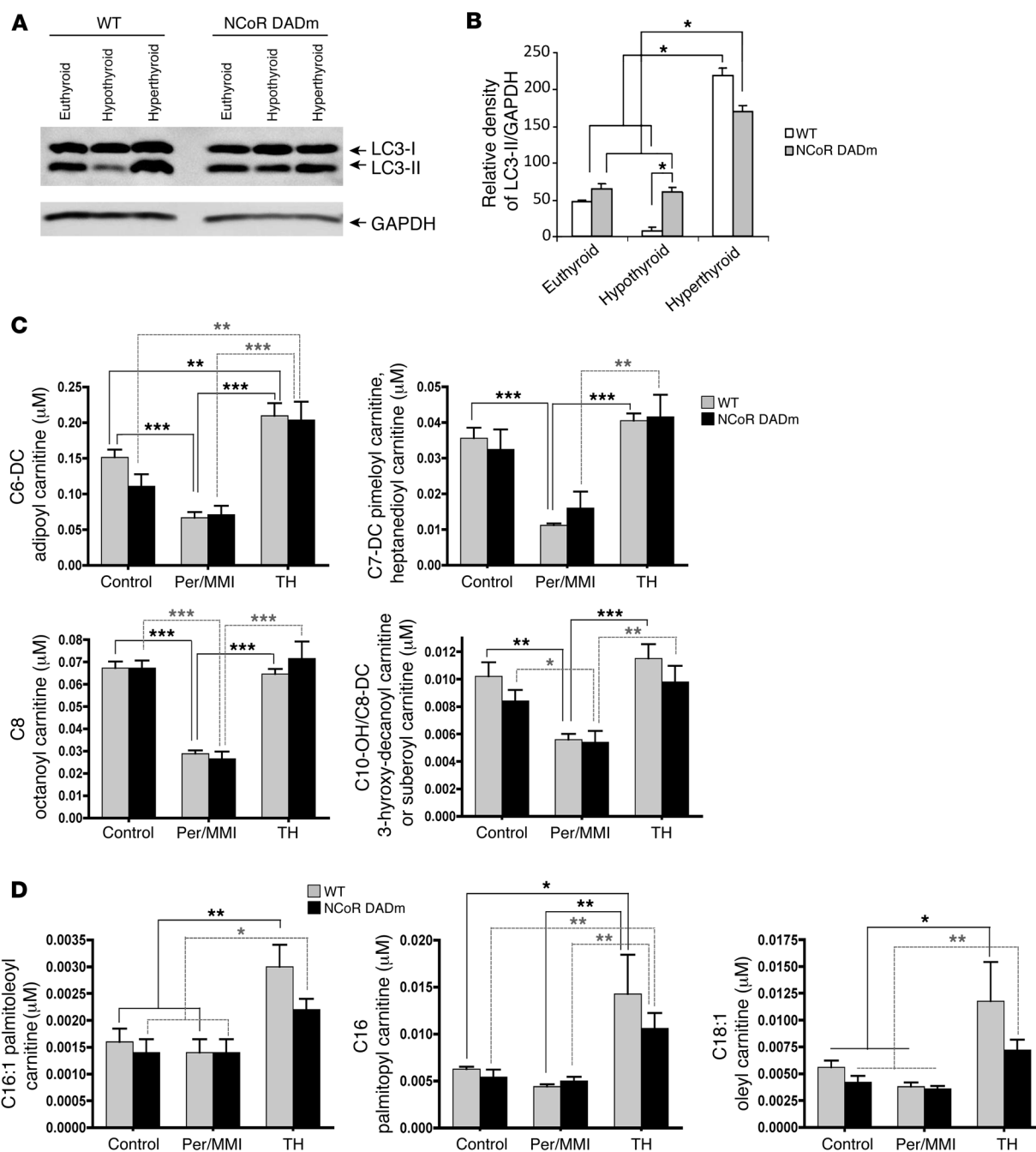


**Figure 9**

NCoR modulates T<sub>3</sub>-mediated autophagy and acylcarnitine levels in vivo. **(A and B)** Immunoblot and densitometric analysis of LC3-II levels in WT and NCoR DADm mice. Female WT and NCoR DADm mice (19 weeks old) were used for the experiment. Fresh drinking water containing 1% perchlorate and 0.05% methimazole was provided daily for 2 weeks to induce hypothyroidism. Fourteen hours before they were killed, all animals were given a subcutaneous injection of vehicle (0.9% saline in 100 μl volume for control and hypothyroid groups or 40.0 μg/100 g T<sub>4</sub> with 4.0 μg/100 g T<sub>3</sub> for hyperthyroid group). \**P* < 0.05; *n* = 3 animals in each group. **(C)** Metabolomic analysis of medium-chain acylcarnitines in the above-described animal groups (*n* = 5; \**P* < 0.05). **(D)** Metabolomic analysis of long-chain acylcarnitines in the above-described animal groups (*n* = 5; \**P* < 0.05; \*\**P* < 0.01; \*\*\**P* < 0.001). Results are expressed as mean ± SEM.

15% v/v methanol). Membranes were blocked in 5% milk and subsequently were incubated in 1% w/v bovine serum albumin in PBST with specific antibodies overnight at 4°C. Membranes were washed 3 times in TBST and subsequently incubated with species-appropriate, peroxidase-conju-

gated secondary antibodies (Santa Cruz Biotechnology Inc.) for 1 hour. Blots were washed 3 times with TBST and once with TBS without Tween and developed using an enhanced chemiluminescence system (GE Healthcare). Densitometry analysis was performed using ImageJ software (NIH).



As recommended by recent reviews on autophagy detection methodology (56–59), we generally used LC3-II/actin ratio as an index of autophagosome formation; however, LC3-II/LC3-I ratio also showed in some of the same figures. Both methodologies gave similar results even though the magnitude of the ratios may be different.

**Immunofluorescence studies.** After treatment, cells were washed in PBS and then fixed with 4% paraformaldehyde for 15 minutes at room temperature. Fixed cells were washed with PBS, permeabilized in 100% methanol for 10 minutes at  $-20^{\circ}\text{C}$ , washed in PBS, and blocked in blocking buffer for 1 hour at room temperature. Cells subsequently were incubated with anti-LC3 antibody overnight at  $4^{\circ}\text{C}$ . After 3 TBST washes, cells were incubated with Alexa Fluor-anti-rabbit antibody (Invitrogen) for 2 hours at room temperature and then washed 3 times in TBST. Coverslips were mounted on slides using Vectashield anti-fade reagent with 4',6-diamidino-2-phenylindole (Invitrogen). Cells were observed under fluorescence or confocal microscopes. For autophagic flux analysis, tandem RFP/GFP-tagged LC3 plasmid (a gift from T. Yoshimori, Osaka University) was transfected into HepG2/TR $\alpha$  cells with Lipofectamine 2000 Transfection Reagent (Invitrogen). Cells were visualized after 48 hours treatment with T<sub>3</sub> (1  $\mu\text{M}$ ) using an LSM710 Carl Zeiss confocal microscope.

**EM.** Cells were seeded onto 4-chambered coverglass (Nalgene-Nunc) at a density of  $2 \times 10^4$  cells/ml (14,000 cells/well). After 72 hours, cells were fixed with 2.5% glutaraldehyde and washed 3 times with PBS. Subsequent post-fixation with 1% osmium tetroxide was followed by dehydration with an ascending series of alcohol before embedding samples in Araldite. Ultrathin sections were cut and doubly stained with uranyl acetate and lead citrate. Images were acquired using the Olympus EM208S transmission electron microscope.

**Knockdown of ATG5 by siRNA and  $\beta$ -hydroxybutyrate measurement.** Stealth siRNA duplex oligoribonucleotides targeting ATG5 (Invitrogen) were resuspended to make a 20- $\mu\text{M}$  solution following the manufacturer's instructions. Transfections were carried out in HepG2/TR $\alpha$  cells using 10 nM of both ATG5 and negative control siRNA (Stealth RNAi siRNA; Invitrogen) and Lipofectamine RNAiMAX (Invitrogen) following the reverse transfection protocol for HepG2 cells. Conditions were optimized with varying ratios of Lipofectamine and RNA as well as different time intervals after the transfections, as determined by immunoblot analysis of ATG5 protein levels. After 24 hours of transfection, cells were subjected to T<sub>3</sub> (1  $\mu\text{M}$ ) and oleic acid (0.5 mM) treatment and consequent  $\beta$ -hydroxybutyrate release in the medium after 48 hours of treatment using a  $\beta$ -hydroxybutyrate assay kit (Abcam).

**Metabolomic analysis.** Hepatic acylcarnitines were measured in liver extracts by previously described methods (60, 61). Briefly, proteins were removed by methanol precipitation and analytes esterified with hot, acidic methanol (acylcarnitines) or *n*-butanol (amino acids). Analysis employed tandem MS with a Quattro Micro instrument (Waters Corporation), and quantification of the "targeted" intermediary metabolites was achieved by addition of stable-isotope internal standards. Total ketone levels were measured in plasma as described (62).

**In vivo ATG5 siRNA treatment and measurement of ketone bodies.** Male C57BL/6 mice (4 to 6 weeks old) receiving T<sub>3</sub> (10  $\mu\text{g}/100$  g BW i.p.) were coadministered 40  $\mu\text{g}$  of ATG5 (5'-ACCGGAAACUCAUGGAAUA-3') or Negative Control siSTABLE siRNA (D-001700-01; Dharmacon) every 24 hours for 3 days via hydrodynamic tail-vein injection protocol using Mirus Bio TransIT-QR Delivery Solution. The non-T<sub>3</sub>-treated control mice and a

group of T<sub>3</sub>-treated mice ( $n = 4$ –5 per group) received an equivalent amount of Negative Control siSTABLE siRNA in TransIT-QR Delivery Solution (Mirus Bio). Serum ketone levels were measured using a  $\beta$ -hydroxybutyrate assay kit (Cayman Chemical).

**Liver microarray and pathway analysis.** Total RNA was extracted from the liver using the RNeasy Tissue Mini Kit (QIAGEN) according to the manufacturer's instructions. Preparation of RNA for hybridization to Affymetrix MoGene 1.0 ST (Affymetrix) and scanning of the arrays were performed by the University of Pennsylvania Microarray Facility (<http://www.bioinformatics.upenn.edu/index.html>) according to the manufacturer's instructions. Robust multiarray averaging (RMA) signal extraction, normalization, and filtering were performed by the University of Pennsylvania Microarray Facility Bioinformatics Group (<http://www.pcbi.upenn.edu/>) using Partek Genomics Suite (Partek). An adjusted *P* value based on the false discovery rate (FDR) was used for filtering. Pathway analysis was done using DAVID Bioinformatics Resources 6.7 (63).

**Calculations and statistics.** Individual culture experiments were performed in duplicate or triplicate and repeated 3 independent times using matched controls; the data were pooled. Results were expressed as mean  $\pm$  SEM. The statistical significance of differences ( $P < 0.05$ ) was assessed by 2-tailed *t* test.

**Study approval.** All mice were maintained according to the *Guide for the Care and Use of Laboratory Animals* (NIH publication no. 1.0.0. Revised 2011), and experiments were approved by the IACUCs at the University of Pennsylvania, the National Cancer Institute, and the Duke-NUS Graduate Medical School.

## Acknowledgments

The authors would like to thank Benjamin A. Bikman, Chui Sun Yap, Brijesh Singh, Guan Yuguang and Sherwin Ying Xie (Cardiovascular and Metabolic Disorders Program, Duke-NUS Graduate Medical School), and Mei Wang (Cancer Stem Cell Program, Duke-NUS Graduate Medical School) for their helpful advice and constructive criticism. This work was supported by grant NIH DK 43806 (to M.A. Lazar), the Nuclear Receptor Signaling Atlas grant NIH U19DK/HL/ES 62434 (to C.B. Newgard and M.A. Lazar), and an American Diabetes Association (ADA) mentored research fellowship (to S.H. You and M.A. Lazar). This work also was supported by Duke-NUS Graduate Medical School Faculty Funds (to P.M. Yen and S.A. Summers) sponsored by the Ministry of Health, Ministry of Education, and Ministry of Trade, Singapore, and A\*StaR.

Received for publication November 28, 2011, and accepted in revised form April 26, 2012.

Address correspondence to: Paul M. Yen, Duke-NUS Graduate Medical School, Laboratory of Hormonal Regulation, CVMD Program, 8 College Road, Singapore 018987. Phone: 65.6516.7332; Fax: 65.6516.7396; E-mail: paul.yen@duke-nus.edu.sg. Or to: Mitchell A. Lazar, University of Pennsylvania, 3400 Civic Center Blvd., Bldg. 421, Translational Research Center, 12-102, Philadelphia, Pennsylvania 19104, USA. Phone: 215.898.0199; Fax: 215.898.5408; E-mail: lazar@mail.med.upenn.edu. Or to: Christopher B. Newgard, Duke University Medical Center, Duke Independence Park Facility, 4321 Medical Park Drive, Durham, North Carolina 27704, USA. Phone: 919.668.6059; Fax: 919.477.0632; E-mail: newga002@mc.duke.edu.

1. Magnus-Levy A. Über den respiratorischen Gaswechsel unter dem Ein fluss der Thyroidea sowie unter verschiedenen pathologischen Zuständen. *Berl Klin Wochenschr.* 1895;32:650–652.
2. Thompson WO, Thompson PK, Brailey AG, Cohen

- AC. The calorigenetic action of thyroxin at different levels of basal metabolism in myxedema. *J Clin Invest.* 1929;7(3):437–463.
3. Landowne M. Specific dynamic action of carbohydrate and of protein in human hypothyroidism

after total ablation of the normal thyroid gland. *J Clin Invest.* 1935;14(5):595–603.

4. Ismail-Beigi F, Bissell DM, Edelman IS. Thyroid thermogenesis in adult rat hepatocytes in primary monolayer culture: direct action of thyroid hor-





1. mone in vitro. *J Gen Physiol.* 1979;73(3):369–383.
5. DeLuise M, Flier JS. Status of the red cell Na,K-pump in hyper- and hypothyroidism. *Metabolism.* 1983;32(1):25–30.
6. Bianco AC, Sheng XY, Silva JE. Triiodothyronine amplifies norepinephrine stimulation of uncoupling protein gene transcription by a mechanism not requiring protein synthesis. *J Biol Chem.* 1988; 263(34):18168–18175.
7. Gong DW, He Y, Karas M, Reitman M. Uncoupling protein-3 is a mediator of thermogenesis regulated by thyroid hormone, beta3-adrenergic agonists, and leptin. *J Biol Chem.* 1997;272(39):24129–24132.
8. Yen PM. Physiological and molecular basis of thyroid hormone action. *Physiol Rev.* 2001;81(3):1097–1142.
9. Ishizuka T, Lazar MA. The nuclear receptor corepressor deacetylase activating domain is essential for repression by thyroid hormone receptor. *Mol Endocrinol.* 2005;19(6):1443–1451.
10. Feng X, Jiang Y, Meltzer P, Yen PM. Thyroid hormone regulation of hepatic genes in vivo detected by complementary DNA microarray. *Mol Endocrinol.* 2000;14(7):947–955.
11. Flores-Morales A, et al. Patterns of liver gene expression governed by TRbeta. *Mol Endocrinol.* 2002; 16(6):1257–1268.
12. Jackson-Hayes L, et al. A thyroid hormone response unit formed between the promoter and first intron of the carnitine palmitoyltransferase-1alpha gene mediates the liver-specific induction by thyroid hormone. *J Biol Chem.* 2003;278(10):7964–7972.
13. Oppenheimer JH, Schwartz HL, Lane JT, Thompson MP. Functional relationship of thyroid hormone-induced lipogenesis, lipolysis, and thermogenesis in the rat. *J Clin Invest.* 1991;87(1):125–132.
14. Liu YY, Brent GA. Thyroid hormone crosstalk with nuclear receptor signaling in metabolic regulation. *Trends Endocrinol Metab.* 2010;21(3):166–173.
15. Singh R, et al. Autophagy regulates lipid metabolism. *Nature.* 2009;458(7242):1131–1135.
16. Cahova M, Dankova H, Palenickova E, Papackova Z, Kazdova L. The autophagy-lysosomal pathway is involved in TAG degradation in the liver: the effect of high-sucrose and high-fat diet. *Folia Biol (Praha).* 2010;56(4):173–182.
17. Ding WX, Li M, Yin XM. Selective taste of ethanol-induced autophagy for mitochondria and lipid droplets. *Autophagy.* 2011;7(2):248–249.
18. Yang L, Li P, Fu S, Calay ES, Hotamisligil GS. Defective hepatic autophagy in obesity promotes ER stress and causes insulin resistance. *Cell Metab.* 2010;11(6):467–478.
19. Amir M, Czaja MJ. Autophagy in nonalcoholic steatohepatitis. *Expert Rev Gastroenterol Hepatol.* 2011;5(2):159–166.
20. Kaushik S, Singh R, Cuervo AM. Autophagic pathways and metabolic stress. *Diabetes Obes Metab.* 2010;12(suppl 2):4–14.
21. Javitt NB. Hep G2 cells as a resource for metabolic studies: lipoprotein, cholesterol, and bile acids. *FASEB J.* 1990;4(2):161–168.
22. Hayashi Y, Yamaguchi S, Pohlenz J, Murata Y, Refetoff S, Seo H. Modification of thyroid hormone and 9-cis retinoic acid signaling by overexpression of their cognate receptors using adenoviral vector. *Mol Cell Endocrinol.* 1997;131(1):59–66.
23. Chen RN, Huang YH, Yeh CT, Liao CH, Lin KH. Thyroid hormone receptors suppress pituitary tumor transforming gene 1 activity in hepatoma. *Cancer Res.* 2008;68(6):1697–1706.
24. Chan IH, Privalsky ML. Isoform-specific transcriptional activity of overlapping target genes that respond to thyroid hormone receptors alpha1 and beta1. *Mol Endocrinol.* 2009;23(11):1758–1775.
25. Nikodem VM, Cheng SY, Rall JE. Affinity labeling of rat liver thyroid hormone nuclear receptor. *Proc Natl Acad Sci U S A.* 1980;77(12):7064–7068.
26. Klionsky DJ, Cuervo AM, Seglen PO. Methods for monitoring autophagy from yeast to human. *Autophagy.* 2007;3(3):181–206.
27. Kimura S, Noda T, Yoshimori T. Dissection of the autophagosome maturation process by a novel reporter protein, tandem fluorescent-tagged LC3. *Autophagy.* 2007;3(5):452–460.
28. Chow VT, Lim SS, Tock EP. The c-erbA beta thyroid hormone receptor. Expression and cDNA sequence analysis of the hormone-binding domain in human cancer cell lines. *Acta Oncol.* 1994;33(5):499–505.
29. Ventura-Holman T, Mamoon A, Maher JF, Subauste JS. Thyroid hormone responsive genes in the murine hepatocyte cell line AML 12. *Gene.* 2007;396(2):332–337.
30. Wang M, et al. A small molecule inhibitor of isoprenylcysteine carboxymethyltransferase induces autophagic cell death in PC3 prostate cancer cells. *J Biol Chem.* 2008;283(27):18678–18684.
31. Biederbick A, Kern HF, Elsasser HP. Monodansylcadaverine (MDC) is a specific in vivo marker for autophagic vacuoles. *Eur J Cell Biol.* 1995;66(1):3–14.
32. DeMartino GN, Goldberg AL. Thyroid hormones control lysosomal enzyme activities in liver and skeletal muscle. *Proc Natl Acad Sci U S A.* 1978; 75(3):1369–1373.
33. Harper ME, Seifert EL. Thyroid hormone effects on mitochondrial energetics. *Thyroid.* 2008; 18(2):145–156.
34. Kaneshige M, et al. Mice with a targeted mutation in the thyroid hormone beta receptor gene exhibit impaired growth and resistance to thyroid hormone. *Proc Natl Acad Sci U S A.* 2000;97(24):13209–13214.
35. Takeda K, Balzano S, Sakurai A, DeGroot LJ, Refetoff S. Screening of nineteen unrelated families with generalized resistance to thyroid hormone for known point mutations in the thyroid hormone receptor beta gene and the detection of a new mutation. *J Clin Invest.* 1991;87(2):496–502.
36. Araki O, Ying H, Zhu XG, Willingham MC, Cheng SY. Distinct dysregulation of lipid metabolism by unliganded thyroid hormone receptor isoforms. *Mol Endocrinol.* 2009;23(3):308–315.
37. Davis PJ, Davis FB, Cody V. Membrane receptors mediating thyroid hormone action. *Trends Endocrinol Metab.* 2005;16(9):429–435.
38. Feng X, Jiang Y, Meltzer P, Yen PM. Transgenic targeting of a dominant negative corepressor to liver blocks basal repression by thyroid hormone receptor and increases cell proliferation. *J Biol Chem.* 2001;276(18):15066–15072.
39. Astapova I, Lee LJ, Morales C, Tauber S, Bilban M, Hollenberg AN. The nuclear corepressor, NCoR, regulates thyroid hormone action in vivo. *Proc Natl Acad Sci U S A.* 2008;105(49):19544–19549.
40. You SH, Liao X, Weiss RE, Lazar MA. The interaction between nuclear receptor corepressor and histone deacetylase 3 regulates both positive and negative thyroid hormone action in vivo. *Mol Endocrinol.* 2010;24(7):1359–1367.
41. Cioffi F, Lanni A, Goglia F. Thyroid hormones, mitochondrial bioenergetics and lipid handling. *Curr Opin Endocrinol Diabetes Obes.* 2010;17(5):402–407.
42. Kuma A, et al. The role of autophagy during the early neonatal starvation period. *Nature.* 2004; 432(7020):1032–1036.
43. Rautou PE, Mansouri A, Lebrec D, Durand F, Valla D, Moreau R. Autophagy in liver diseases. *J Hepatol.* 2010;53(6):1123–1134.
44. Tacke F, Trautwein C. Controlling autophagy: a new concept for clearing liver disease. *Hepatology.* 2011;53(1):356–358.
45. Shibata M, et al. LC3, a microtubule-associated protein 1A/B light chain3, is involved in cytoplasmic lipid droplet formation. *Biochem Biophys Res Commun.* 2010;393(2):274–279.
46. Egan DF, et al. Phosphorylation of ULK1 (hATG1) by AMP-activated protein kinase connects energy sensing to mitophagy. *Science.* 2011;331(6016):456–461.
47. Liu YL, Yang PM, Shun CT, Wu MS, Weng JR, Chen CC. Autophagy potentiates the anti-cancer effects of the histone deacetylase inhibitors in hepatocellular carcinoma. *Autophagy.* 2010;6(8):1057–1065.
48. Fang S, et al. Corepressor SMRT promotes oxidative phosphorylation in adipose tissue and protects against diet-induced obesity and insulin resistance. *Proc Natl Acad Sci U S A.* 2011;108(8):3412–3417.
49. Mauvezin C, et al. The nuclear cofactor DOR regulates autophagy in mammalian and *Drosophila* cells. *EMBO Rep.* 2010;11(1):37–44.
50. Pihlajamaki J, et al. Thyroid hormone-related regulation of gene expression in human fatty liver. *J Clin Endocrinol Metab.* 2009;94(9):3521–3529.
51. Liangpunsakul S, Chalasani N. Is hypothyroidism a risk factor for non-alcoholic steatohepatitis? *J Clin Gastroenterol.* 2003;37(4):340–343.
52. Postic C, Girard J. Contribution of de novo fatty acid synthesis to hepatic steatosis and insulin resistance: lessons from genetically engineered mice. *J Clin Invest.* 2008;118(3):829–838.
53. Baehrecke EH. Autophagy: dual roles in life and death? *Nat Rev Mol Cell Biol.* 2005;6(6):505–510.
54. Kumar A, et al. Hyperthyroidism induces apoptosis in rat liver through activation of death receptor-mediated pathways. *J Hepatol.* 2007;46(5):888–898.
55. Kamimoto T, et al. Intracellular inclusions containing mutant alpha1-antitrypsin Z are propagated in the absence of autophagic activity. *J Biol Chem.* 2008;281(7):4467–4476.
56. Mizushima N, Yoshimori T. How to interpret LC3 immunoblotting. *Autophagy.* 2007;3(6):542–545.
57. Klionsky DJ, et al. Guidelines for the use and interpretation of assays for monitoring autophagy in higher eukaryotes. *Autophagy.* 2008;4(2):151–175.
58. Kimura S, Fujita N, Noda T, Yoshimori T. Monitoring autophagy in mammalian cultured cells through the dynamics of LC3. *Methods Enzymol.* 2009;452:1–12.
59. Barth S, Glick D, Macleod KF. Autophagy: assays and artifacts. *J Pathol.* 2010;221(2):117–124.
60. An J, et al. Hepatic expression of malonyl-CoA decarboxylase reverses muscle, liver and whole-animal insulin resistance. *Nat Med.* 2004;10(3):268–274.
61. Ferrara CT, et al. Genetic networks of liver metabolism revealed by integration of metabolic and transcriptional profiling. *PLoS Genet.* 2008;4(3):e1000034.
62. Newgard CB, et al. A branched-chain amino acid-related metabolic signature that differentiates obese and lean humans and contributes to insulin resistance. *Cell Metab.* 2009;9(4):311–326.
63. Huang da W, Sherman BT, Lempicki RA. Systematic and integrative analysis of large gene lists using DAVID bioinformatics resources. *Nat Protoc.* 2009;4(1):44–57.